Supporting Information for:

Dual-Plasmonic Au and $CoNiO_2$ co-sensitized ZnO Membrane: Photothermal Effect Promotes Charge Separation for Enhanced Visible-Light-Infrared-Driven CO_2 Reduction

Erhan Qin[a], Mingke Zhang[a], Cuiyu Gao[a], Lili Yang[a, b], Yuan Teng[c], Xin Li[a, b*], Binrong Li[d*], Maobin Wei[a, b], Jinghai Yang[a, b*]

[a] *Key Laboratory of Functional Materials Physics and Chemistry of the Ministry of Education, Jilin Normal University, Siping 136000, Jilin, China*

[b] *National Demonstration Center for Experimental Physics Education, Jilin Normal University, Siping 136000, China*

[c] *College of Chemistry and Chemical Engineering, Jishou University, Jishou 416000, China*

[d] *National and Local Joint Engineering Laboratory of Municipal Sewage Resource Utilization Technology, School of Environmental Science and Engineering, Suzhou University of Science and Technology, Suzhou 215009, PR China*

E-mail: xlwl@jlnu.edu.cn

1. Characterization

X-ray diffraction (XRD) analysis was conducted to characterize the crystal structure of powdered samples, using a D/max2500PC rotating anode diffractometer with Cu Kα radiation and point detectors in Bragg-Brentano geometry. The diffractometer operated at 40 kV and 200 mA, with a scanning rate set to 5°/min. Morphological observations were carried out via transmission electron microscopy (TEM, JEOL JEM-HR2100), while surface topography and elemental distribution were examined using field-emission scanning electron microscopy (FE-SEM, JEOL 7800F) equipped with elemental mapping functionality. X-ray photoelectron spectroscopy (XPS, Escalab 250 XI) was employed to investigate the surface chemical states of the samples, with the C 1s peak at 284.6 eV used for calibration. Optical properties were evaluated through photoluminescence (PL) spectroscopy using a Horiba Jobin Yvon Fluorolog-3 system. All PL measurements were performed at room temperature, with a 375 nm laser as the excitation source; the excitation and emission wavelengths were fixed at 360 nm and 435 nm, respectively, and a 395 nm filter was applied. UV-Vis absorption spectra (200–800 nm) were recorded using a Shimadzu UV-2700 spectrometer. *In-situ* Fourier transform infrared spectroscopy (FTIR, Nicolet iS50) was utilized to monitor the CO_2 PR process. Prior to testing, the catalyst was pretreated by vacuum drying at 120°C for 2 h; the reaction system was then assembled with 50 mg of catalyst and 2 mL of H_2O under a N_2-purged atmosphere. Photoelectrochemical measurements were performed on a CHI 660B electrochemical workstation using a standard three-electrode cell (Ag/AgCl as the reference electrode). The measurements included transient photocurrent response, electrochemical impedance spectroscopy (EIS, conducted in 0.1 M Na_2SO_4 electrolyte), linear sweep voltammetry, and Mott-Schottky analysis. Isotopic verification experiments were carried out using ^{13}C-labeled gas chromatography-mass spectrometry (MS, Agilent 7890B-5977B).

2. Photocatalytic activity measurement

The photocatalytic CO_2 reduction (CO_2 PR) performance was evaluated in a custom-designed gas-solid reactor (300 mL) without sacrificial agents, illuminated by a 300 W Xe arc lamp (PLS-SXE300D) under full-spectrum irradiation. The catalyst (2×2 cm^2 in size) was mounted at the middle of the reactor, with 50 mL deionized water added to the reactor bottom to provide a humid environment. Prior to the reaction, high-purity CO_2 (99.999%) was continuously purged into the reactor for 30 min to thoroughly displace the air and ensure a CO_2-saturated atmosphere.

After 4 h of irradiation, the gaseous products were quantified using a Shimadzu GC-2014 gas chromatograph equipped with flame ionization and thermal conductivity detectors. For the cycle stability test, the catalyst was retrieved from the reactor after each run, rinsed with water three times, and dried. Considering the potential slight catalyst loss during washing, a parallel cycle experiment was conducted under identical conditions: the recovered catalyst was weighed after drying, and the lost portion was compensated before redispersing it into the original reaction system to maintain consistent reaction conditions. Isotopic verification experiments were performed with $^{13}CO_2$/Ar mixtures (*v*/*v* = 1:4) following the same reaction protocol to confirm the carbon source of the generated products and exclude the interference of external carbon impurities. Specifically, prior to the isotopic experiment, the reactor was first evacuated to a vacuum state using a vacuum pump to remove any residual air and carbon-containing impurities. Subsequently, 10 mL of $^{13}CO_2$/argon mixture (with 99.9% purity of $^{13}CO_2$) was injected into the reactor, ensuring that the atmosphere inside the reactor is completely composed of the isotopic mixture and free from contamination by ordinary $^{12}CO_2$. The catalyst, reactor setup, irradiation conditions (300 W Xe lamp), and reaction duration (4 h) were kept identical to those of the standard CO_2 PR experiment. After the reaction, the gaseous products were collected and analyzed using gas chromatograph, with an additional mass spectrometer (MS) connected to the gas chromatograph for precise detection of the isotopic composition of the products (e.g., ^{13}CO, $^{13}CH_4$ if generated), which directly confirms that the products are derived from the photoreduction of the fed $^{13}CO_2$ rather than other carbonaceous impurities in the system.

Blank control experiments were systematically conducted to eliminate the influence of external factors (e.g., reactor materials, light-induced reactions without catalyst, water vapor) on the CO_2 PR performance and product generation. Three groups of parallel blank experiments were designed as follows: (1) Blank experiment without catalyst: The reactor was assembled according to the standard protocol, with 50 mL deionized water added to the bottom, but no catalyst was mounted. High-purity CO_2 (99.999%) was purged for 30 min to achieve a saturated atmosphere, followed by 4 h of full-spectrum irradiation using the 300 W Xe-lamp. After the reaction, gaseous products were detected using the same GC method to verify whether CO_2 can be reduced by light alone without the catalyst. (2) Blank experiment without light irradiation: The reactor was loaded with the catalyst (2×2 cm^2) and 50 mL deionized water, purged with high-purity CO_2 for 30 min, and then placed in a dark environment (completely shielded from light) for 4 h under the same temperature and pressure conditions as the

standard experiment. Gaseous products were detected afterward to rule out the possibility of thermal catalytic reaction or spontaneous CO_2 conversion without light. (3) Blank experiment without CO_2: The reactor was loaded with the catalyst and 50 mL deionized water, and high-purity Ar (99.999%) was purged for 30 min to displace air, followed by 4 h of full-spectrum irradiation. Product detection was performed to confirm that no carbon-containing products were generated from the catalyst itself or other carbon impurities in the system. All blank experiments were repeated three times to ensure the reliability of the results, and no detectable gaseous products were observed in any of the blank groups, confirming that the catalytic products in the standard experiment are indeed derived from the photocatalytic reduction of CO_2 by the catalyst under light irradiation.

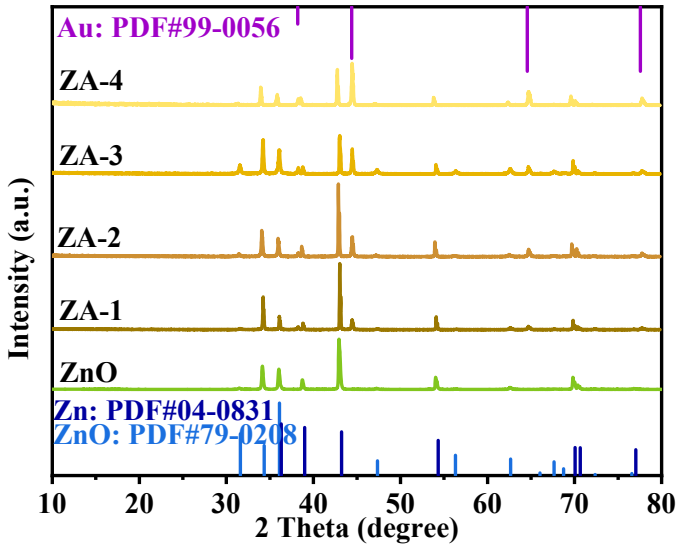

Fig. S1 The XRD patterns of ZnO, ZA-1, ZA-2, ZA-3, and ZA-4 samples.

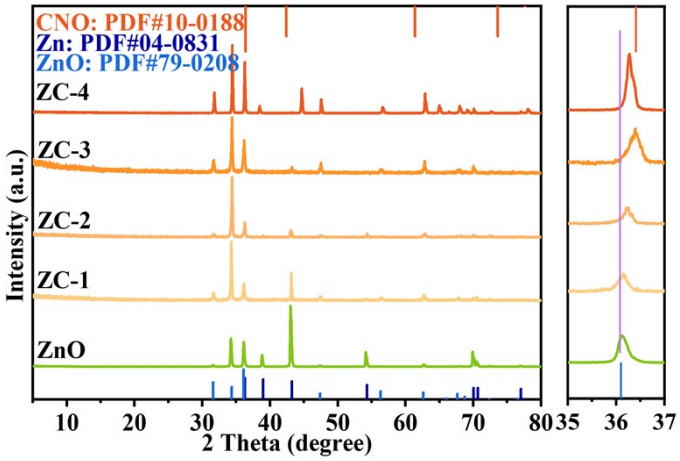

Fig. S2 The XRD patterns of ZnO, ZC-1, ZC-2, ZC-3, and ZC-4 samples.

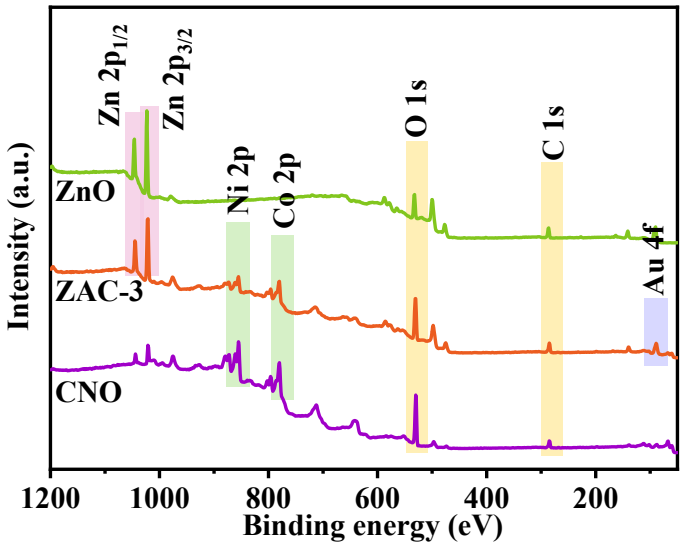

Fig. S3 XPS survey spectra for CNO, ZAC-3 and ZnO samples.

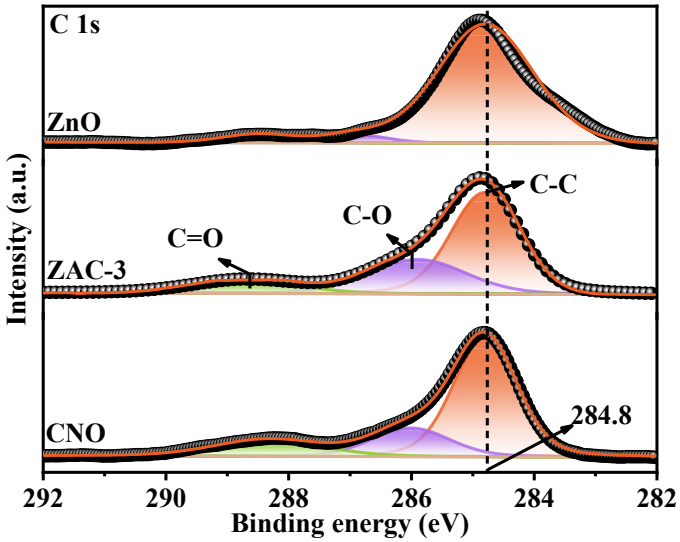

Fig. S4 High-resolution XPS spectra of C 1s for CNO, ZAC-3 and ZnO samples.

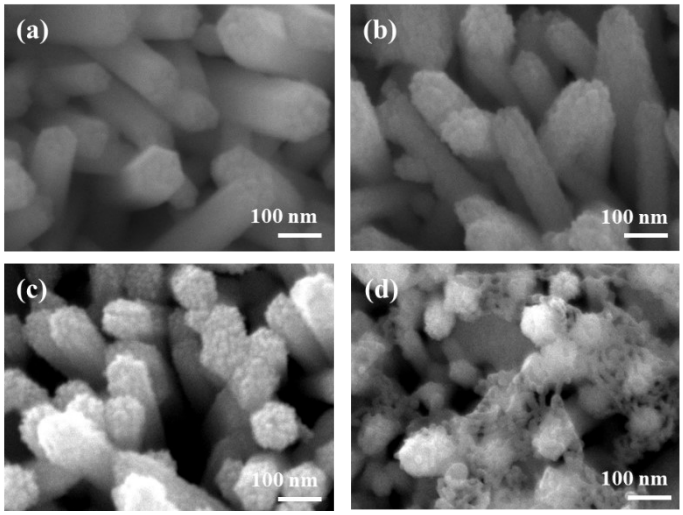

Fig. S5 SEM images of (a) ZA-1, (b) ZA-2, (c) ZA-3, and (d) ZA-4 samples.

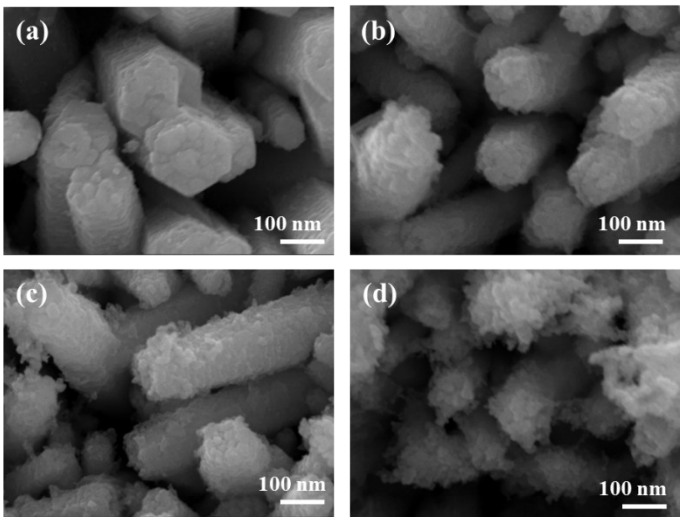

Fig. S6 SEM images of (a) ZC-1, (b) ZC-2, (c) ZC-3, and (d) ZC-4 samples.

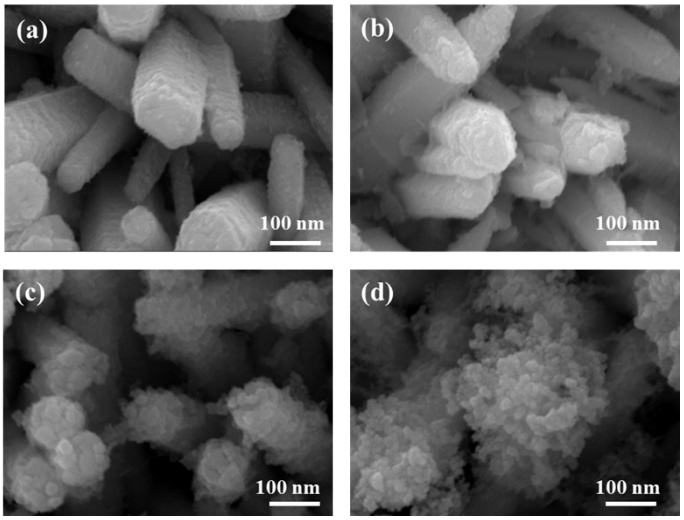

Fig. S7 SEM images of (a) ZAC-1, (b) ZAC-2, (c) ZAC-3, and (d) ZAC-4 samples.

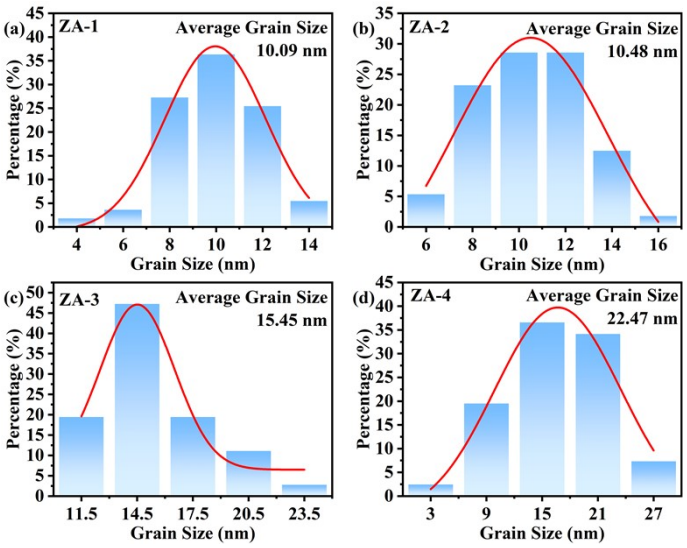

Fig. S8 Particle size distribution statistics of ZA-X samples

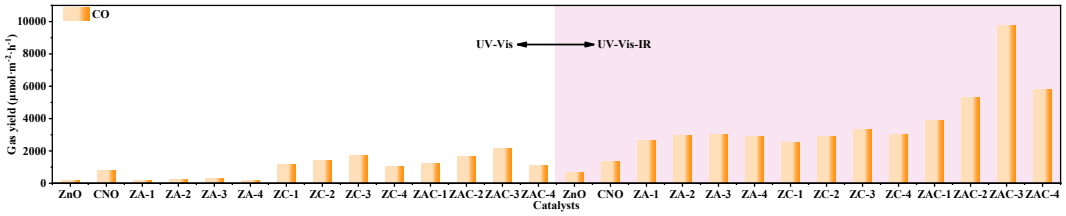

Fig. S9 Product yield of PTCR catalyst.

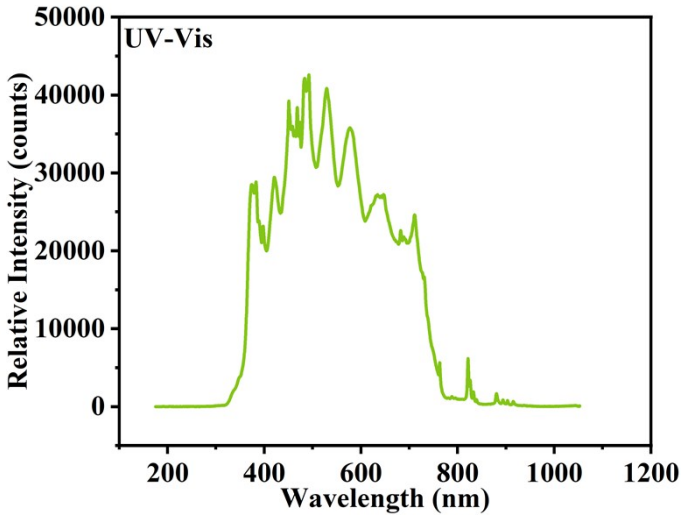

Fig. S10 Spectral distribution of Xenon lamp under UV-Vis irradiation.

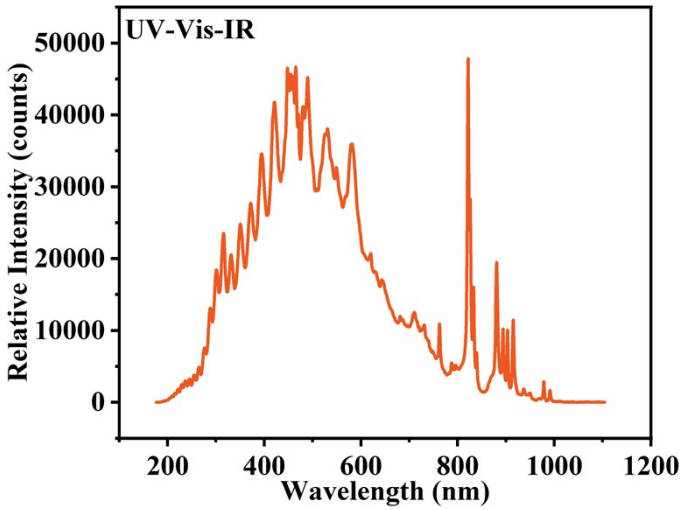

Fig. S11 Spectral distribution of Xenon lamp under UV-Vis-IR irradiation.

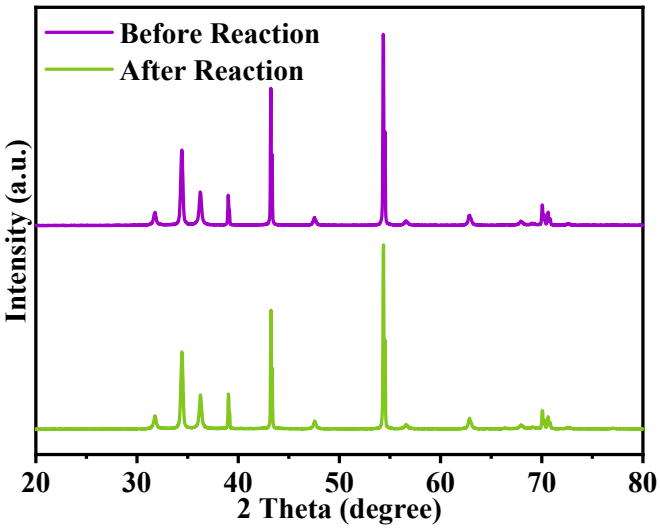

Fig. S12 XRD comparison before and after reaction for ZAC-3 sample.

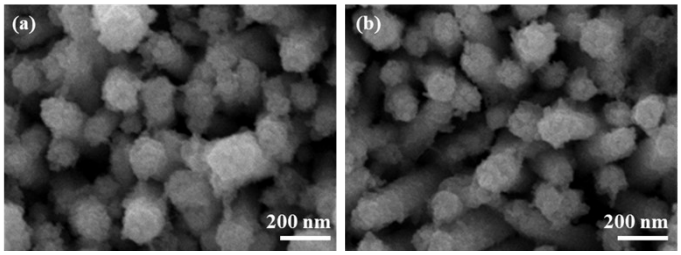

Fig. S13 SEM images comparison before and after reaction for ZAC-3 sample.

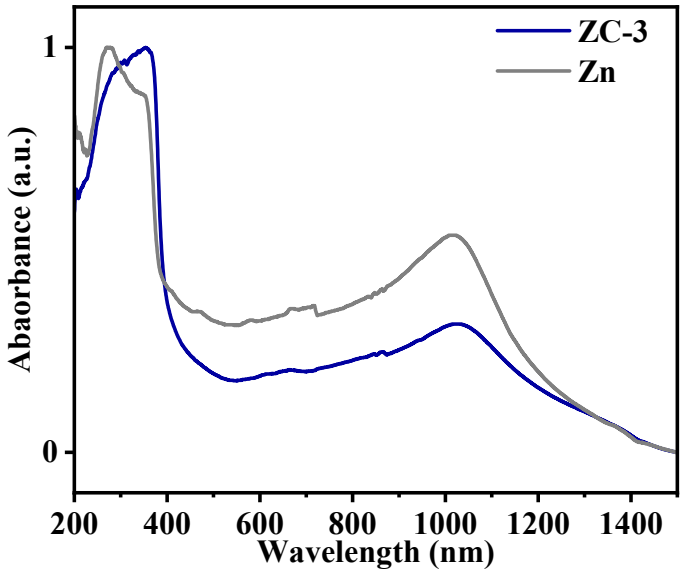

Fig. S14 Normalized UV–Vis absorption spectra of ZC-3 and Zn.

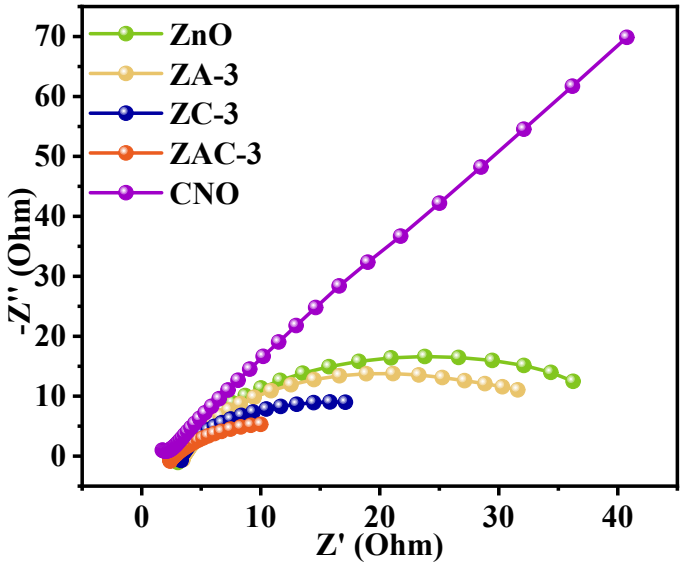

Fig. S15 EIS of ZnO, CNO, ZA-3, ZC-3, and ZAC-3 samples.

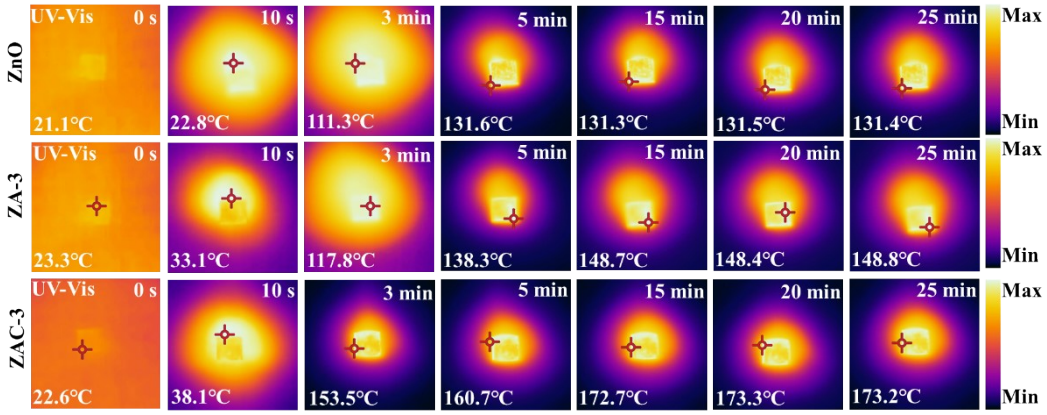

Fig. S16 Infrared thermal images of ZnO, ZA-3, and ZAC-3 samples under UV-Vis xenon lamp irradiation.

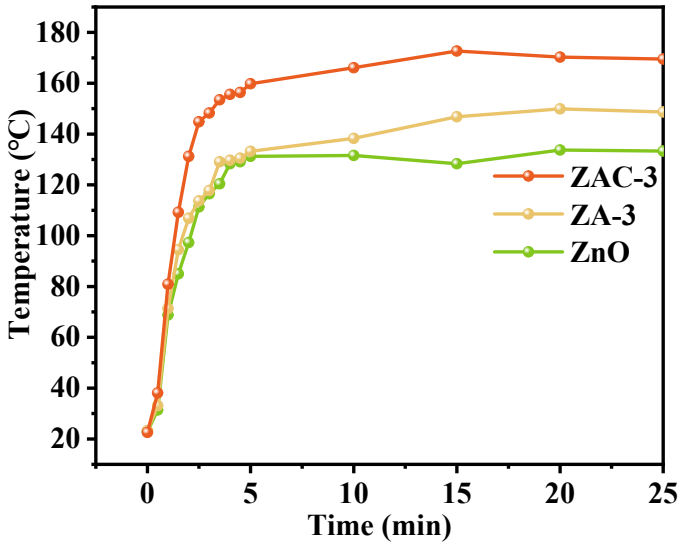

Fig. S17 Point-line graphs of temperature changes of ZAC-3, ZA-3 and ZnO samples under UV-Vis irradiation for 25 min.

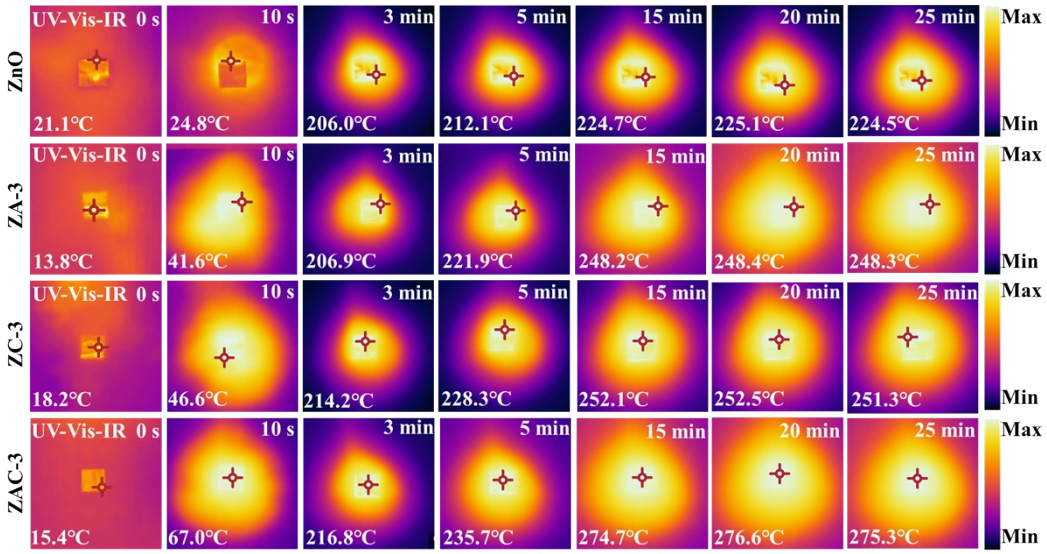

Fig. S18 Infrared thermal images of ZnO, ZA-3, ZC-3, and ZAC-3 samples under UV-Vis-IR xenon lamp irradiation.

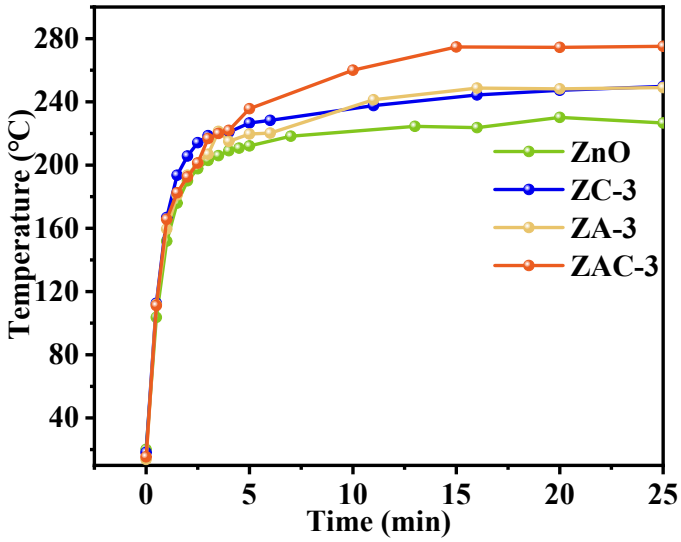

Fig. S19 Point-line graphs of temperature changes of ZAC-3, ZA-3, ZC-3, and ZnO samples under UV-Vis-IR irradiation for 25 min.

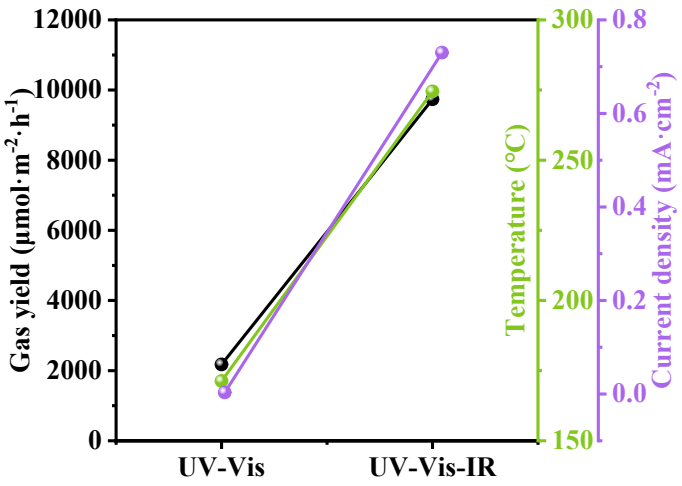

Fig. S20 Line-scatter plots of CO yield, photothermal temperature, and carrier concentration of ZAC-3 under different light irradiation conditions.

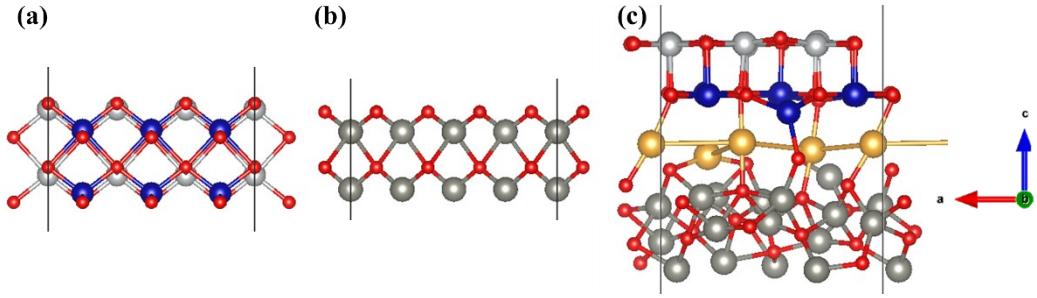

Fig. S21 DFT calculation models constructed based on TEM analysis (a) CNO; (b) ZnO; (c) ZnO/Au/CNO ternary heterojunction.

To ensure the rationality of the calculation and the authenticity of the experiment, combined with the TEM characterization results, the representative (111) crystal plane of CNO and the stable (002) crystal plane of ZnO were selected for modeling. Au nanoparticles were anchored in a monodisperse form at the interface between the ZnO (002) crystal plane and the CNO (111) crystal plane, constructing a ZnO/Au/CNO ternary heterojunction DFT model consistent with the structure of the experimental sample, which provides a reliable structural basis for the subsequent calculations of CO_2 activation, charge transfer and reaction free energy.

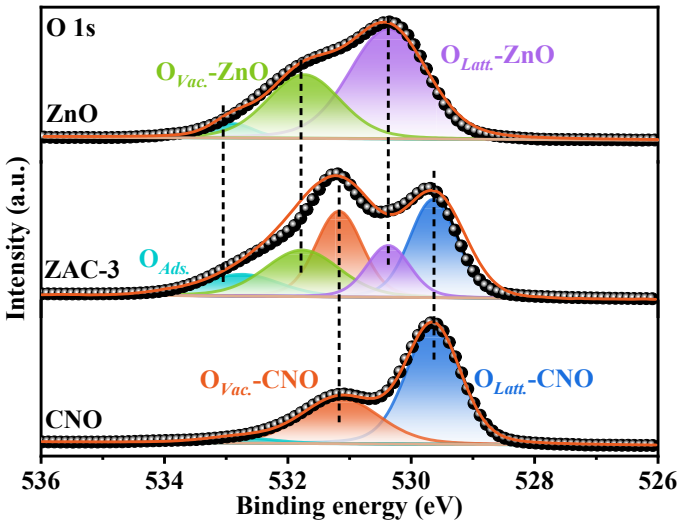

Fig. S22 O 1s XPS spectra of samples.

Table S1 The reaction barrier of each step in CO_2 photoreduction of ZAC-3 sample.

CO generation	Free energy (eV)	ΔG (eV)
Slab+*CO_2	0.00	
↓	↓	0.23
Slab+*COOH	0.23	
↓	↓	-0.54
Slab+*CO	-0.31	
↓	↓	0.07
CO	-0.24	

Table S2 The reaction barrier of each step in CO_2 photoreduction of CNO sample.

CO generation	Free energy (eV)	ΔG (eV)
Slab*CO_2	0.00	
↓	↓	0.54
Slab+*COOH	0.54	
↓	↓	-0.74
Slab+*CO	-0.20	
↓	↓	0.44
CO	0.22	